JOURNAL OF VIROLOGY, Nov. 2010, p. 11089–11100 Vol. 84, No. 21
0022-538X/10/$12.00 doi:10.1128/JVI.01383-10

Pathogenesis and Immune Response of Crimean-Congo Hemorrhagic Fever Virus in a STAT-1 Knockout Mouse Model▽†

Dennis A. Bente,[1]* Judie B. Alimonti,[1,3] Wun-Ju Shieh,[4] Gaëlle Camus,[1,2] Ute Ströher,[1,3] Sherif Zaki,[4] and Steven M. Jones[1,2,3]

Special Pathogens Program, National Microbiology Laboratory, Public Health Agency of Canada, Winnipeg, Manitoba, Canada[1]; Department of Immunology, University of Manitoba, Winnipeg, Manitoba, Canada[2]; Department of Medical Microbiology, University of Manitoba, Winnipeg, Manitoba, Canada[3]; and Infectious Disease Pathology Branch, Centers for Disease Control and Prevention, Atlanta, Georgia[4]

Received 2 July 2010/Accepted 19 August 2010

Tick-borne Crimean-Congo hemorrhagic fever virus (CCHFV) causes a severe hemorrhagic syndrome in humans but not in its vertebrate animal hosts. The pathogenesis of the disease is largely not understood due to the lack of an animal model. Laboratory animals typically show no overt signs of disease. Here, we describe a new small-animal model to study CCHFV pathogenesis that manifests clinical disease, similar to that seen in humans, without adaptation of the virus to the host. Our studies revealed that mice deficient in the STAT-1 signaling molecule were highly susceptible to infection, succumbing within 3 to 5 days. After CCHFV challenge, mice exhibited fever, leukopenia, thrombocytopenia, and highly elevated liver enzymes. Rapid viremic dissemination and extensive replication in visceral organs, mainly in liver and spleen, were associated with prominent histopathologic changes in these organs. Dramatically elevated proinflammatory cytokine levels were detected in the blood of the animals, suggestive of a cytokine storm. Immunologic analysis revealed delayed immune cell activation and intensive lymphocyte depletion. Furthermore, this study also demonstrated that ribavirin, a suggested treatment in human cases, protects mice from lethal CCHFV challenge. In conclusion, our data demonstrate that the interferon response is crucial in controlling CCHFV replication in this model, and this is the first study that offers an in-depth *in vivo* analysis of CCHFV pathophysiology. This new mouse model exhibits key features of fatal human CCHF, proves useful for the testing of therapeutic strategies, and can be used to study virus attenuation.

Crimean-Congo hemorrhagic fever (CCHF) is a severe, often fatal tick-borne zoonosis caused by the arbovirus Crimean-Congo hemorrhagic fever virus (CCHFV), which is a member of the genus *Nairovirus* within the family *Bunyaviridae* (35). The geographic range of CCHFV is the most extensive of the medically significant tick-borne viruses, and it is the second-most-widespread of all medically important arboviruses after dengue virus (35). There are reports of viral isolation and/or disease from more than 30 countries in Africa, Asia, Southeast Europe, and the Middle East (10). Outbreaks are usually sporadic, with only a few cases; however, recent increases in the number of cases in the Balkan area, Turkey, and Southwest Asia demonstrate the imminent public health impact of this reemerging disease. The potential influence of climate change on the spread of the disease has been suggested (27). In addition, its potential use as an agent for bioterrorism is of concern.

CCHFV circulates in a tick-vertebrate-tick cycle. Ixodid (hard) ticks, especially those of the genus *Hyalomma*, are both a reservoir and a vector for the virus. CCHFV infection has been detected in numerous wild and domestic animals, such as cattle, goats, sheep, and hares, all of which serve as amplifying hosts for the virus. Remarkably, CCHFV produces no disease in its natural hosts; however, it causes severe disease in humans (35). Transmission to humans occurs through contact with infected animal blood or ticks or from one infected human to another by contact with infectious blood or body fluids (10, 35). Human infection is usually characterized by a sudden onset of symptoms, such as high fever, headache, myalgia, and petechial rash, frequently followed by a hemorrhagic state, and can progress to multiorgan failure (11). Leukopenia, thrombocytopenia, and elevated liver enzymes are hallmarks of the disease (7). The case fatality rate in outbreaks has been very broad, ranging between 5 and 70% (35). At this point, there is no commercially available vaccine. Ribavirin has been suggested as a treatment, and its efficacy has been investigated in observational studies; however, evidence of its efficacy is controversial in part due to the lack of randomization of these studies and the small number of patients studied (11).

The pathogenesis of CCHF is poorly understood due to the lack of a suitable animal model to study the disease, the fact that it occurs mainly in regions lacking modern medical infrastructure, and because its high virulence requires work to be performed under biosafety level 4 (BSL-4) containment. Most of what is known today is derived from human case studies and some *in vitro* experiments, and much is extrapolated from what is known from other viral hemorrhagic fevers. A broad range of domestic and laboratory animals have been tested as potential animal models since the first isolation of the virus in 1956 (24, 37). Experimentally infected animals, such as calves, horses, guinea pigs, hamsters, and rabbits, develop little or no

* Corresponding author. Mailing address: Special Pathogens Program, National Microbiology Laboratory, 1015 Arlington Street, Winnipeg, Manitoba R3E 3R2, Canada. Phone: (204) 789-7027. Fax: (204) 789-2140. E-mail: Dennis.Bente@phac-aspc.gc.ca.

▽ Published ahead of print on 25 August 2010.

† The authors have paid a fee to allow immediate free access to this article.

viremia and high levels of neutralizing antibodies but do not display clinical signs of disease (24, 29). Unlike most hemorrhagic fever viruses, CCHFV has not been found to cause disease in commonly used species of nonhuman primates (14, 30). Adult immunocompetent mice are not susceptible to CCHFV infection and show no signs of disease (30). On the other hand, an infant mouse infection model has been reported with high virus titers in blood and liver (33). Although there is evidence of systemic viral dissemination and infection of macrophages in these mice, which is consistent with the paradigm of viral hemorrhagic fever, virus could not be isolated from the spleen where large numbers of mononuclear phagocytes reside (18). Additionally, it is not very practical to use a neonate mouse in a BSL-4 setting in regard to animal husbandry and the difficulty in frequent collection of samples for pathogenesis studies.

Earlier studies have demonstrated that human interferons (IFNs) have an antiviral effect against bunyaviruses (23). Moreover, the results of *in vitro* studies have shown that the IFN response plays a crucial role in controlling CCHFV replication, and a recent study demonstrates that IFN receptor knockout (KO) mice are highly susceptible to CCHFV infection (3–5).

In this study, we show that a functional IFN response is critical in controlling CCHFV replication. We used mice with a homozygous disruption of the signal transducer and activator of transcription 1 (STAT1) protein, a key player in the IFN signaling pathway (22). There are three types of IFNs, type I (alpha interferon [IFN-α] and IFN-β), type II (IFN-γ), and type III (IFN-λ). In the case of IFN-α/β and IFN-λ stimulation, although utilizing different receptor complexes, STAT1 and STAT2 are activated and translocated to the nucleus and, consequently, bind to promoters of the IFN response genes. In contrast, IFN-γ triggers the activation of STAT1 but not STAT2. Therefore, STAT1 KO mice exhibit selective signaling defects in their response to all three types of IFNs that lead to a complete abolishment of the intracellular IFN response (2).

Here, we demonstrate that STAT1 knockout mice are highly susceptible to even low doses of CCHFV challenge. We also demonstrate that many features of human disease can be found in this new mouse model. Additionally, we show that ribavirin protects animals from CCHFV challenge.

MATERIALS AND METHODS

Mice. This study used 3- to 6-week-old 129S6/SvEv-*Stat1*^{tm1Rds} mice (STAT129) and congenic control mice (WT129) (Taconic, Germantown, NY) (22) of both sexes. Mice were randomized, and subdermal transponders measuring body temperature (Biomedic Data Solutions, Seaford, DE) were implanted. Following implantation, the animals were moved into the BSL-4 and allowed to acclimate for 7 days before challenge. Mice were kept under barrier conditions in environmentally enriched sterile housing with food and water *ad libitum*. All animal procedures were conducted according to the guidelines of the Canadian Council on Animal Care and performed in accordance with institutional regulations and after review and approval by the Animal Care Committee of the Canadian Science Centre for Human and Animal Health.

Virus and cells. CCHFV strain IbAr 10200 was kindly provided by Michael Holbrook (University of Texas Medical Branch, Galveston, TX). IbAr 10200 had a titer of 4×10^5 PFU per ml (6.2×10^8 genome equivalents/ml), had been passaged 10 times in suckling mice and 3 times in SW-13 cells, and was not plaque purified. Viral stocks were sequenced based on the protocol of Deyde et al. (8), and the viral sequence was confirmed by comparison to GenBank reference entries (accession numbers AY389508, AF467768, and CHU88410). SW-13 cells (ATCC catalog number CCL-105) passaged 42 to 46 times were maintained in L-15 medium containing 10% heat-inactivated fetal bovine serum (FBS), 100 mM L-glutamine, 50 U/ml penicillin, 50 μg/ml streptomycin (all from Sigma, St. Louis, MO). Virus stock and inocula tested negative for pyrogen contamination with a Pyrogent plus test kit (Lonza, Wakersville, MD).

Median lethal dose challenge and pathogenesis experiments. For the median (50%) lethal dose (LD_{50}) experiment, virus inoculates containing 1,000, 100, 10, 1, and 0.1 PFU in 200 μl (1.55×10^6, 1.55×10^5, 1.55×10^4, 1.55×10^3, and 1.55×10^2 GEQ [genome equivalence]) were administered to groups of six STAT129 and WT129 mice intraperitoneally (i.p.). Mice were observed twice daily, and clinical score, body temperature, and weight change were recorded daily. Percent survival, geometric mean time to death (GMD), and percent weight change were calculated.

For pathogenesis experiments, 15 STAT129 mice and 15 WT129 mice were administered i.p. 100 PFU (1.55×10^5 GEQ) of CCHFV in 200 μl of modified Eagle's medium (MEM). Mock-infected animals received 200 μl of MEM medium (Sigma). An i.p. route was chosen since it is an established technique in the BSL-4 animal protocols. Groups of 5 CCHFV-infected mice and 3 mock-infected mice were euthanized at 1, 2, and 3 days postinfection (dpi) by isoflurane overdose. Blood was collected by cardiac puncture in EDTA-and-serum microtainers (Becton-Dickinson), and plasma and serum were separated by centrifugation. From the median lethal dose experiment, a scoring sheet for behavioral and physical changes following intraperitoneal injection of the virus was developed, and criteria for humane endpoint euthanasia were defined. Animals were observed and scored for each parameter. Normal behavior and no clinical signs of disease were scored 0. Reduced exploratory behavior and/or slight lethargy were scored 1. Lethargy, piloerection, and hunched posture were scored 2. Immobility, apathy, severely hunched posture, and labored breathing were scored 3. Found dead in cage was scored 4. When the humane endpoint was reached (score 3), animals were euthanized by inhalation of isoflurane followed by cervical dislocation.

Ribavirin treatment. Ribavirin was used in the form of Virazol (Valeant, Montreal, Canada). Virazol powder was dissolved in sterile, endotoxin-free cell culture water, and the concentration was adjusted according to mouse weight to give a final concentration of 100 mg/kg of body weight of ribavirin per mouse. Two hundred microliters of solution was given i.p. at either 1 h after CCHFV challenge (treatment group A) or 24 h after CCHFV challenge (treatment B). Animals in both groups received ribavirin daily from then on until day 14 postchallenge.

Plaque assay. Plaque assay was performed on Sw-13 cells as previously described, and the results expressed as PFU per ml (34).

Immunophenotyping. The spleen from each mouse was homogenized with a 50-μm Medicon in a BD Medimachine with 1.5 ml RPMI. A million splenocytes were washed once in phosphate-buffered saline (PBS), resuspended in 100 μl PBS, and blocked with 1 μg Fc block (BD catalog number 553140) for 10 min at room temperature before the addition of a 100-μl master mix of antibodies for 30 min at 4°C. Two panels of antibodies were used: panel 1 contained CD19 fluorescein isothiocyanate (FITC), CD49b phycoerythrin (PE), CD3 peridinin chlorophyll protein (PerCP)-Cy5.5, CD25 PE-Cy7, CD8 allophycocyanin (APC), and CD4 Alx700; panel 2 contained CD86 FITC, CD3 PE, CD19 PE, CD49b PE, CD11b PerCP-Cy5.5, CD11c PE-Cy7, CD80 APC, I-A/I-E Alx700, and F4/80 Pacific blue. After 30 min at 4°C, red blood cells were lysed by adding 250 μl of PharMLyse (BD) for 15 min at room temperature. After centrifugation at 300 × *g* for 10 min, the pellet was washed with 1 ml of Dulbecco's PBS (Invitrogen) and then resuspended in 1 ml PBS, 4% paraformaldehyde (PFA). Samples were acquired and analyzed on a BD LSRII flow cytometer using Diva fluorescence-activated cell sorting (FACS) software, version 5.0.2 (Becton Dickinson). Prior to runs, 100 μl of Flowcount fluorospheres (Beckman Coulter) was added for determination of absolute counts. For the dendritic cell (DC) population, the lineage-negative (Lin^-) markers excluded CD3, CD19, and CD49b.

Cytokine detection. To determine cytokine levels in the blood of the mice, EDTA microtainers filled with blood were centrifuged for 3 min at 10,000 × *g*, and plasma was collected. Twenty-microliter amounts of plasma were run in duplicates with a multiplex Milliplex map mouse cytokine kit (Millipore Corp., MA) according to the manufacturer's instructions. The kit simultaneously quantifies granulocyte-macrophage colony-stimulating factor (GM-CSF), IFN-γ, interleukin-1β (IL-1β), IL-2, IL-4, IL-6, IL-10, IL-12(p70), CCL-2, and tumor necrosis factor (TNF). The samples were run on a LiquiChip (Qiagen, Valencia, CA) and analyzed using Luminex 100 IS software (Luminex). IFN-α and IFN-β were measured in plasma of mice using a VeriKine mouse interferon alpha and beta enzyme-linked immunosorbent assay (ELISA) kit (PBL Interferon Source, NJ), following the manufacturer's instructions.

Antibody response. The CCHFV-specific IgM antibody response in plasma of infected STAT129 and WT129 mice was quantified using Euroimmun's indirect

immunofluorescence test (Euroimmun, Lübeck, Germany) according to the manufacturer's instructions.

Histopathology and immunohistochemistry. At necropsy, liver, spleen, kidney, lung, and brain of infected STAT129 and WT129 animals, as well as mock-infected STAT129 animals, were harvested and fixed with neutral-buffered formalin (10%). Routine paraffin embedding and hematoxylin-eosin staining was performed on all sections. An immunohistochemical assay (IHC) was performed as previously described (6).

RNA extraction and quantitative real-time RT-PCR. To determine viremia levels, 140 μl of EDTA blood was mixed with 560 μl of AVL buffer (QIAamp viral RNA mini kit; Qiagen). RNA was isolated following the manufacturer's instructions. To determine viral titers in tissues, a 3-mm by 3-mm piece of tissue was removed during necropsy and homogenized using metal beads (Tissue Lyser, Qiagen) in RLT buffer (Qiagen), and RNA was extracted using an RNeasy kit (Qiagen) according to the manufacturer's instructions. CCHFV-specific quantitative real-time reverse transcription (RT)-PCR was performed as previously described (36). Viral titers were reported as the genome equivalence (GEQ). To normalize viral titers in tissues to the total amount of RNA, a housekeeping-gene RT-PCR targeting the glyceraldehyde 3-phosphate dehydrogenase (GAPDH) gene was established. Genome equivalents were normalized to 1 μg of RNA for each tissue. Predeveloped mouse GAPDH hydrolysis probes and TaqMan gene expression assays (both from Applied Biosystems, Foster City, CA) were used. Assays were run on a StepOnePlus (Applied Biosystems) and analyzed with StepOne software, version 2.1.

Hematology and clinical chemistry. Twenty-five-microliter amounts of EDTA blood were used for complete blood counts. All cell counts were quantified using an ABC Vet hematology analyzer (Horiba ABX, France) equipped with software to measure white blood cell count, red blood cell count, platelet counts, hemoglobin concentration, hematocrit, mean corpuscular volume, mean corpuscular hemoglobin, and mean corpuscular hemoglobin concentration. One hundred-microliter amounts of serum were used for clinical chemistry. Analysis was performed using a VetScan2 chemistry analyzer (Abaxis, Inc., Sunnyvale, CA), which provides a diagnostic panel that includes albumin, alkaline phosphatase, alanine aminotransferase, amylase, total bilirubin, blood urea nitrogen, calcium, creatinine, glucose, and potassium.

Statistical analysis. All data were analyzed with GraphPad Prism software (Graphpad Software, Inc., San Diego, CA). For survival analysis, Kaplan-Meier survival curves were analyzed by log-rank test. The median lethal dose was calculated by logistic regression. An unpaired Student's *t* test was used to determine significant differences between CCHFV-infected and mock-infected animals in hematology, clinical chemistry, body temperature, weight changes, and cytokines and for the FACS analysis between various days. The minimum significance threshold for two-tailed *P* values was set to 0.05 before each experiment. The *P* value results are flagged with a single asterisk when the *P* value is less than 0.05, with two asterisks when the *P* value is less than 0.01, and with three asterisks when the *P* value is less than 0.001.

RESULTS

Mice lacking the STAT1 signaling protein are highly susceptible to CCHFV infection. To determine if the STAT1 signaling protein plays a critical role in controlling CCHFV susceptibility, mice lacking the STAT1 protein (STAT129) and congenic wild-type mice (WT129) were challenged with CCHFV. To calculate the LD_{50}, groups of 6 mice, 3 to 6 weeks old, were inoculated i.p. with 10-fold serial dilutions, starting with 1,000 PFU and going down to 0.1 PFU (1.55×10^6 to 1.55×10^2 GEQ), of CCHFV strain IbAr 10200 (Fig. 1A). As expected, adult WT129 mice were resistant to CCHFV infection, exhibiting neither morbidity nor mortality. STAT129 mice were highly susceptible to the virus and showed 100% mortality at dilutions as low as 10 PFU. Animals challenged with 1,000, 100, and 10 PFU succumbed to the disease between 3 and 5 days postinfection (dpi). There was a dose dependency in regard to the geometric mean time to death (Fig. 1A). The LD_{50} was calculated by logistic regression as 4 PFU. These results indicate that a deficiency in STAT1-dependent IFN signaling makes mice highly susceptible to CCHFV infection.

STAT129 mice succumb to CCHFV infection rapidly, with a distinct clinical presentation and changes in hematology and clinical chemistry. To determine the pathogenesis throughout the infection, STAT129 mice and WT129 mice were challenged with 100 PFU (1.55×10^5 GEQ) of CCHFV i.p. and monitored daily. STAT129 mice uniformly exhibited the first clinical signs of illness by 3 dpi, which manifested as lethargy, piloerection, and hunched posture. The animals deteriorated rapidly, becoming immobile and weak, and were typically euthanized at 4 dpi when reaching the predefined scoring endpoint. Importantly, none of the CCHFV-infected STAT129 mice developed any clinical signs typically associated with neurologic disease, such as ataxia, paresis, or hind-limb paralysis. This differs drastically from the existing neonate animal model, in which encephalitic paralysis is the major clinical sign following i.p. inoculation (33).

The body temperature in CCHFV-infected STAT129 mice peaked at 2 dpi (Fig. 1B) (mean temperature was 1.65°C higher than that of mock-infected and WT129 mice) without hyperthermic animals exhibiting any clinical signs at this time point. At 3 dpi, animals became hypothermic (mean body temperature 35.21°C) and showed a mean weight loss of 7.1% (Fig. 1B). Body temperature and weight continued to decrease at 4 dpi with a terminal mean temperature of 27°C and mean weight loss of 12.4%. There was no weight loss or temperature rise in CCHFV-infected WT129 mice or mock-infected STAT129 mice.

Hematologic analysis revealed leukopenia and thrombocytopenia in CCHFV-infected STAT129 animals (Fig. 1D and E). White blood cell and platelet counts decreased in CCHFV-infected mice compared to the levels in mock-infected animals on day 1 postinfection and dipped on day 2, while increasing slightly on day 3. However, since hematocrit (Fig. 1F) remained stable throughout the course of infection, a decrease in these two cell populations was not due to a general blood cell loss. In addition, serum levels of liver transaminase alanine aminotransferase (ALT) were measured as an indicator of liver damage (Fig. 1C). Serum ALT levels increased 10-fold by day 3 in CCHFV-infected STAT129 mice compared to the levels in mock-infected STAT129 mice. This feature is clearly indicative of severe hepatic damage. No changes in hematology or clinical pathology were observed in CCHFV-infected WT129 mice.

CCHFV initially replicates in blood, liver, and spleen and, consequently, spreads systemically. In order to determine where CCHFV initially replicates and what organs are the major site of replication, we next investigated CCHFV replication in whole blood and peripheral tissues, namely, liver, spleen, lung, kidney, and brain, at 1 to 3 dpi by quantitative real-time RT-PCR. We were able to detect virus in whole blood of CCHFV-infected STAT129 mice as early as 1 dpi with a mean value of 6.55×10^6 GEQ/ml (Fig. 2A). The mean virus load increased drastically to 1.57×10^9 GEQ/ml at 2 dpi, and viremia peaked at 3 dpi with 7.32×10^9 GEQ/ml, consistent with the morbidity results. Viremia was only detectable in 3 of the 5 CCHFV-infected WT129 mice at 1 dpi, with a mean viral load of 1.14×10^3 GEQ/ml, and was not detectable at 2 and 3 dpi (Fig. 2A). We also looked at infectious titers in some of the blood samples by plaque titration assay (data not shown). The infectious titers correlated strongly with the GEQ; however,

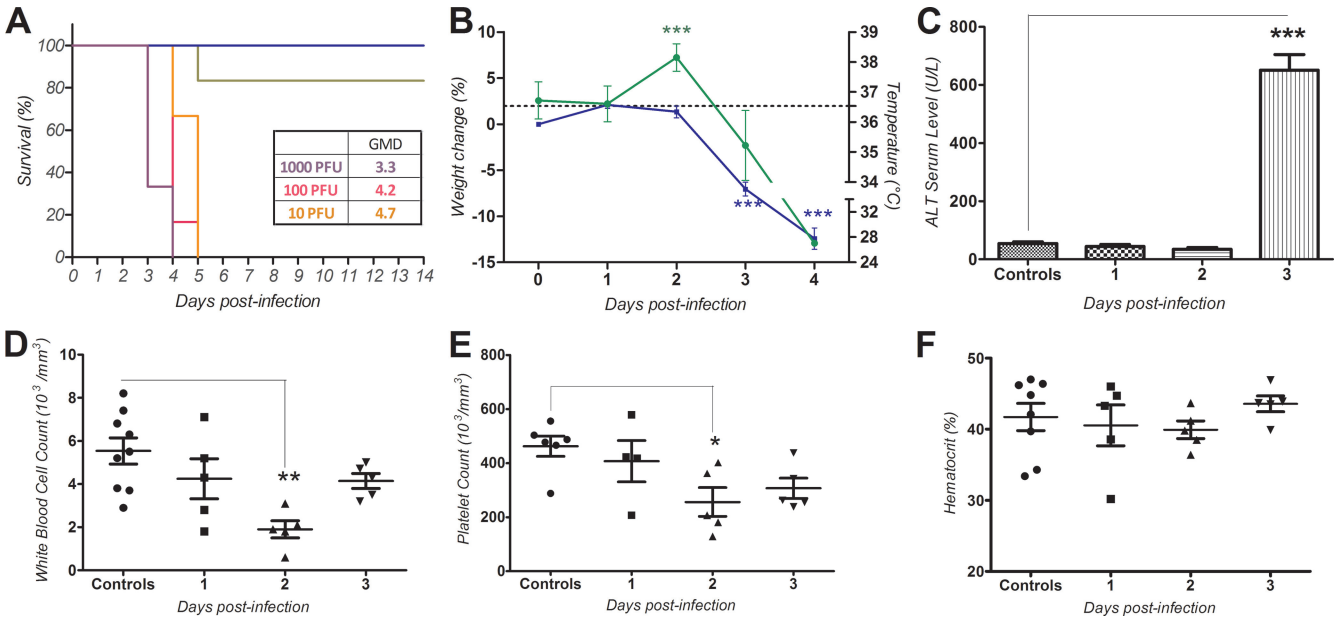

FIG. 1. Survival and clinical parameters following CCHFV challenge. (A) Survival curve of STAT129 mice challenged with serial dilutions of CCHFV. Adult STAT129 mice ($n = 6$ per group) were challenged intraperitoneally with 1,000 PFU (purple), 100 PFU (pink), 10 PFU (orange), 1 PFU (green), or 0.1 PFU (blue) of CCHFV IbAr 10200. Animals succumbed to disease between day 3 and day 5 postinfection. Geometric mean time to death (GMD) was calculated in days. The median lethal dose was 4 PFU. WT129 mice challenged with CCHFV did not succumb to infection (data not shown). (B) Body temperature and weight changes throughout the course of infection. Body temperature (green) and weight change (blue) were monitored over 5 days in STAT129 mice challenged with 100 PFU of CCHFV IbAr 10200 intraperitoneally ($n = 12 \pm$ standard error of the mean). Mice succumbed to disease on day 4 postinfection. Average temperature of mock-infected STAT129 mice (dotted line, $n = 12$) was 36.53°C ± 0.53°C (standard deviation). STAT129 mice challenged with CCHFV showed a highly significant increase in body temperature on day 2 postinfection compared to that of mock-infected mice. Body temperature then dropped to 35.21°C ± 1.14°C on day 3 postinfection, but the difference from the temperature of mock-infected mice was not statistically significant ($P = 0.223$). Mice had lost 7.05% ± 0.72% weight at 3 dpi and 12.43% ± 1.15% on day 4. There was no weight loss or rise in temperature in mock-infected STAT129 or CCHFV-infected WT129 mice (data not shown). (C to F) Hematology and clinical chemistry of CCHFV-infected animals: liver transaminase ALT (C), white blood cell counts (D), platelet counts (E), and hematocrit (F) were measured on days 1, 2, and 3 postinfection in infected and mock-infected (control) animals (means ± standard errors). No significant variation was detected in mock-infected animals; therefore, the results at the 3 time points were pooled (controls). Infected STAT129 mice showed a significant drop in white blood cell counts and platelets on day 2 postinfection compared to the results for the control animals. Hematocrit (F) remained stable throughout the course of infection. Serum levels of liver transaminase ALT (C) increased 10-fold on day 3 compared to the levels in mock-infected animals. The two-tailed P values are indicated as follows: *, $P \leq 0.05$; **, $P \leq 0.01$; ***, $P \leq 0.001$.

the infectious titers were 3 logs lower than the GEQ values. We speculate that the generation of defective interfering particles might explain the discrepancy of low titer but high RNA content.

All five tissues in infected STAT129 and WT129 mice tested at 1 dpi were below the assay's detection limit (Fig. 2B). In STAT129 mice, all liver and spleen samples, as well as 3 out of 5 lung samples, were positive by 2 dpi. At 3 dpi, the titers of liver and spleen samples went up 2 logs and 1 log, respectively. All lung and kidney and 3 out of 5 brain samples were positive by 3 dpi. In WT129 mice, only on day 2 postinfection were 3 out of 5 spleen samples positive (Fig. 2B). All other tissue samples were below the detection limit of the assay. It was not possible to perfuse mice when tissues were harvested; therefore, some of the virus detected in tissue might be blood borne.

CCHFV causes prominent histopathologic changes in liver and spleen of STAT129 mice. Gross examination of organs from CCHFV-infected STAT129 mice revealed discolored liver and spleen, serosal petechia, and intestinal hyperemia by 3 dpi (Fig. 3A to C), whereas organs of mock-infected animals (Fig. 3A) and WT129 mice (data not shown) appeared normal. No hemorrhages were observed in any of the organs of the infected STAT129 mice. When tissues of CCHFV-infected STAT129 mice were trimmed, the liver texture appeared brittle and white pulp in the spleen was diminished. Liver, spleen, kidney, lung, and brain tissues were harvested from CCHFV-infected and mock-infected STAT129 mice at 1, 2, and 3 dpi. Kidney, lung, and brain tissues of CCHFV-infected STAT129 mice were histologically indistinguishable from mock-infected tissues at all time points (data not shown). However, prominent histopathologic changes were observed in liver and spleen tissues in CCHFV-infected STAT129 mice by 3 dpi (Fig. 4A to F), coincident with mice becoming moribund and at the peak level of liver transaminase ALT in the bloodstream (Fig. 1B and C). At 3 dpi, liver sections showed multiple foci of hepatocellular necrosis (Fig. 4A to C). Histopathologic changes in the spleen consisted of prominent follicular lymphocyte depletion accompanied by karyorrhectic debris (Fig. 4D to F). IHC was conducted on the 5 harvested tissues (see above) to locate viral antigen. Viral antigen could be detected in the spleen and liver of CCHFV-infected STAT129 mice by 3 dpi (Fig. 4G to I). IHC on liver sections showed scattered granular staining in hepatocytes and was mainly associated with foci of hepatocel-

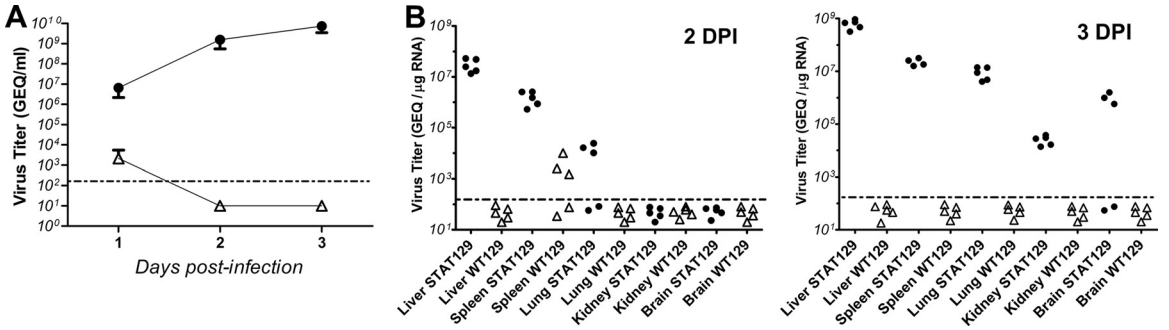

FIG. 2. Viremia levels and tissue titers. STAT129 mice and WT129 mice were inoculated intraperitoneally with 100 PFU of CCHFV IbAr 10200. Virus was detected and quantified in whole blood and organs on days 1, 2, and 3 postinfection by quantitative real-time RT-PCR using a recombinant RNA standard for absolute quantification and reported as genome equivalents (GEQ). (A) Viral load in whole blood was determined. Virus was detected in CCHFV-infected STAT129 mice ($n = 5$ for each time point) on days 1, 2, and 3 postinfection (mean + standard error). In WT129 mice, CCHFV was detected on day 1 postinfection. Virus levels in samples on days 2 and 3 dpi were below the detection limit (dot-dash line; 3×10^2 GEQ/ml). (B) Virus titers were measured in tissues. Liver, spleen, lung, kidney, and brain of infected STAT129 mice and WT129 mice ($n = 5$ for each tissue) were harvested on days 1, 2, and 3 postinfection. Genome equivalents were normalized to 1 μg of RNA for each tissue by quantitative real-time RT-PCR targeting the housekeeping gene GAPDH. All samples were below the detection limit (dot-dash line; 2.5×10^2 GEQ/μg) on day 1.

lular necrosis. Occasional viral antigen could be detected in Kupffer cells and the endothelial lining of sinusoids (Fig. 4I).

CCHFV infection induces a delayed and aberrant immune response. Due to the high levels of apoptosis seen in many hemorrhagic fevers and the possibility of certain leukocyte populations correlating with death, we examined the percentages and activation levels of different lymphocyte, macrophage, and dendritic cell (DC) subpopulations by flow cytometry in the spleen during the course of infection. The blood was not examined as there was not enough available to perform all of the experiments in this study. The overall percentage of $CD3^+$ cells decreased significantly on day 3 postinfection, while the other lymphocytes either remained the same throughout ($CD3^+$ $CD4^+$ T helper cells) or showed a trend toward increasing percentages ($CD3^+$ $CD8^+$ cytotoxic T lymphocytes [CTL] and $CD19^+$ B cells) on day 3 or 2, respectively (Fig. 5A). The most significant increases in percentage occurred in the NK ($CD3^-$ $49b^+$) and NKT-like ($CD3^+$ $49b^+$) populations at 3 dpi. In order to determine if these lymphocytes were being activated, the levels of CD25 were examined. All populations demonstrated a significant increase in the percentage of $CD25^+$ cells at 3 dpi, with the NK populations and NKT-like populations activated a day earlier, before increasing 6.7- or 3-fold, respectively, over the levels in control samples at 3 dpi. In addition to the lymphocytes, the antigen-presenting cells (APC) were also assessed (Fig. 5B). Since macrophages and DC have an important role as APC in the early stages of an infection, their percentages and levels of activation were determined. The percentage of DC (Lin^- $CD11c^+$) initially decreased on day 2 postinfection before increasing on day 3. Meanwhile, the percentages of the two splenocyte macrophage populations ($F4/80^+$ and $CD11b^+$) remained fairly stable before increasing 5- and 4-fold, respectively, on day 3 postinfection. As APCs are important for the activation of other lymphocytes, the upregulation of the specific costimulatory molecules CD80, CD86, and major histocompatibility complex class II (MHC-II) (I-A/I-E) was monitored. CD80 and CD86 increased significantly on day 2 or 3 postinfection in all three APC populations. However, there were no changes in the levels of MHC-II on the DC and F4/80 macrophage populations in comparison to the levels on the CD11b macrophages, which saw an increase in MHC-II at 3 dpi. Overall, the most significant changes in the percentages of the leukocyte populations were generally found in the NK and APC subpopulations on day 3 postinfection. Nevertheless, there were indications that all populations were undergoing some level of activation.

The loss of lymphocytes is a common feature in several viral hemorrhagic fevers, and thus, an absolute count was performed by flow cytometry on various splenocyte populations (Fig. 5A). Although there appeared to be changes in the number of cells on day 3 postinfection for each population, none of the changes were statistically significant due to the high variability arising from the additional steps required for the processing of splenocytes as opposed to blood samples. The decrease in cell number would coincide with the prominent lymphocyte depletion previously seen in the histopathology results. However, despite these difficulties, there were large and significant changes in the $CD25^+$ activation levels of the NK and NKT-like cells, suggesting that there was an early increase in the number of innate cells. A similar trend was seen with the APCs. There is an initial increase in the number of DC and macrophages responding to the infection, but instead of having a sustained response throughout the infection, they decrease in numbers on day 3postinfection. The same holds true for the activation markers as well. Hence, even though activation of many of the splenocyte populations is occurring, it appears that the overall cell numbers are decreasing fairly rapidly.

Next, we analyzed the IgM antibody levels in infected STAT129 and WT129 mice at 3 dpi. As expected, there were no detectable IgM antibody levels in either group. Since the STAT129 mice succumbed to the disease on day 4 postinfection, it was not possible to study their immune response at a later time point. IgM was detectable in WT129 mice when measured on day 10 postinfection (1:60 titer).

We also measured plasma levels of IFN-α, IFN-β, and 10 different proinflammatory cytokines in CCHFV-infected and

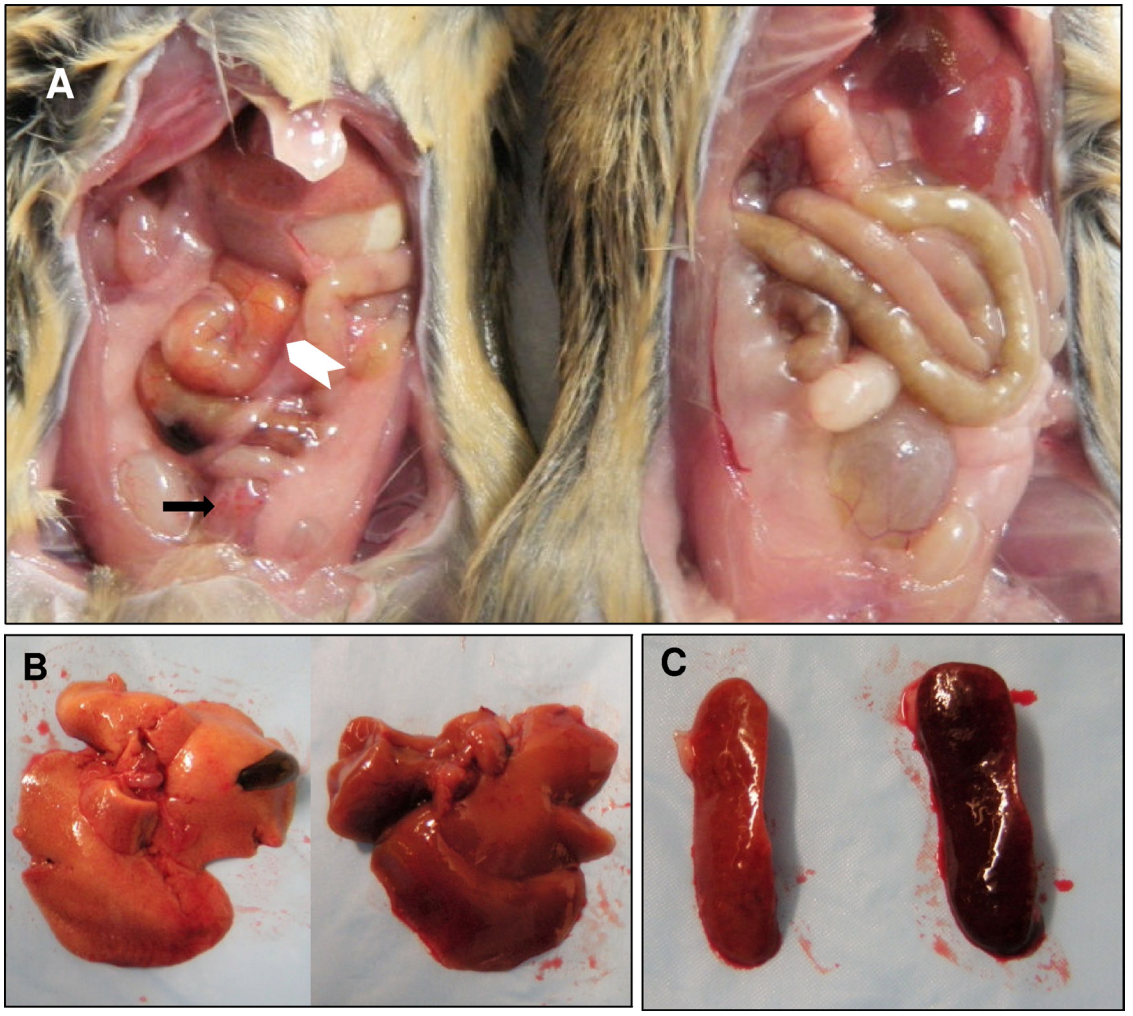

FIG. 3. Gross pathology findings in STAT129 mice. (A) *In situ* picture of organs in CCHFV-infected animals (left) and mock-infected animals (right). Findings included intestinal hyperemia with injected blood vessels (white arrow) and serosal petechia on bladder (black arrow). No hemorrhaging was observed in any of the animals. (B and C) Liver (B) and spleen (C) of CCHFV-infected animals (left) were discolored compared to those of mock-infected animals (right).

mock-infected STAT129 mice, as well as in CCHFV-infected WT129 mice, at 1, 2, and 3 dpi. IFN-α and IFN-β were significantly elevated in CCHFV-infected WT129 mice compared to the levels in mock-infected STAT129 mice at 2 dpi (Fig. 6A) but returned to background values on day 3. High levels of IFN-α and IFN-β were detected in CCHFV-infected STAT129 mice at 2 and 3 dpi that were significantly elevated compared to the levels in mock-infected STAT129 mice (Fig. 6A) and were up to 10 times higher than the levels in CCHFV-infected WT129 mice at 2 dpi. Among 10 different proinflammatory cytokines analyzed, GM-CSF, IL-2, IL-4, and IL-12(p70) were not significantly elevated when the results for CCHFV-infected STAT129 mice were compared to the results for the mock-infected controls. The remaining cytokines, CCL-2, IFN-γ, IL-1β, IL-6, IL-10, and TNF, were significantly elevated and had high plasma levels (Fig. 6B). Three cytokines, namely, IFN-γ, IL-1β, and IL-6, peaked on day 2 postinfection and decreased by day 3. CCL-2, TNF, and IL-10 increased on day 2 postinfection but peaked on day 3 (Fig. 6B). None of the proinflammatory cytokines was significantly elevated when the results for CCHFV-infected WT129 mice were compared to the results for mock-infected STAT129 mice (data not shown).

Ribavirin is protective but is virus dose dependent. In order to examine whether ribavirin protects mice from morbidity and mortality after CCHFV infection, we challenged STAT129 mice with a high virus dose, 250 times the LD_{50} (1,000 PFU), and a low virus dose, 2.5 times the LD_{50} (10 PFU). Each of the virus dose groups was treated with two different ribavirin treatment regimes. Treatment A consisted of 100 mg/kg of ribavirin given i.p. 1 h postinfection and then daily until day 14 postinfection. The early treatment was designed to mimic postexposure treatment after a needle stick injury. Treatment B consisted of 100 mg/kg of ribavirin i.p. 24 h postinfection and then given daily until 14 dpi. When we challenged STAT129 mice with 1,000 PFU, 60% of the animals receiving treatment A survived (Fig. 7A), displaying a low grade of lethargy on days 4 and 7 postinfection but no other clinical signs. The remaining 40% exhibited clinical signs at 7 dpi and succumbed to disease

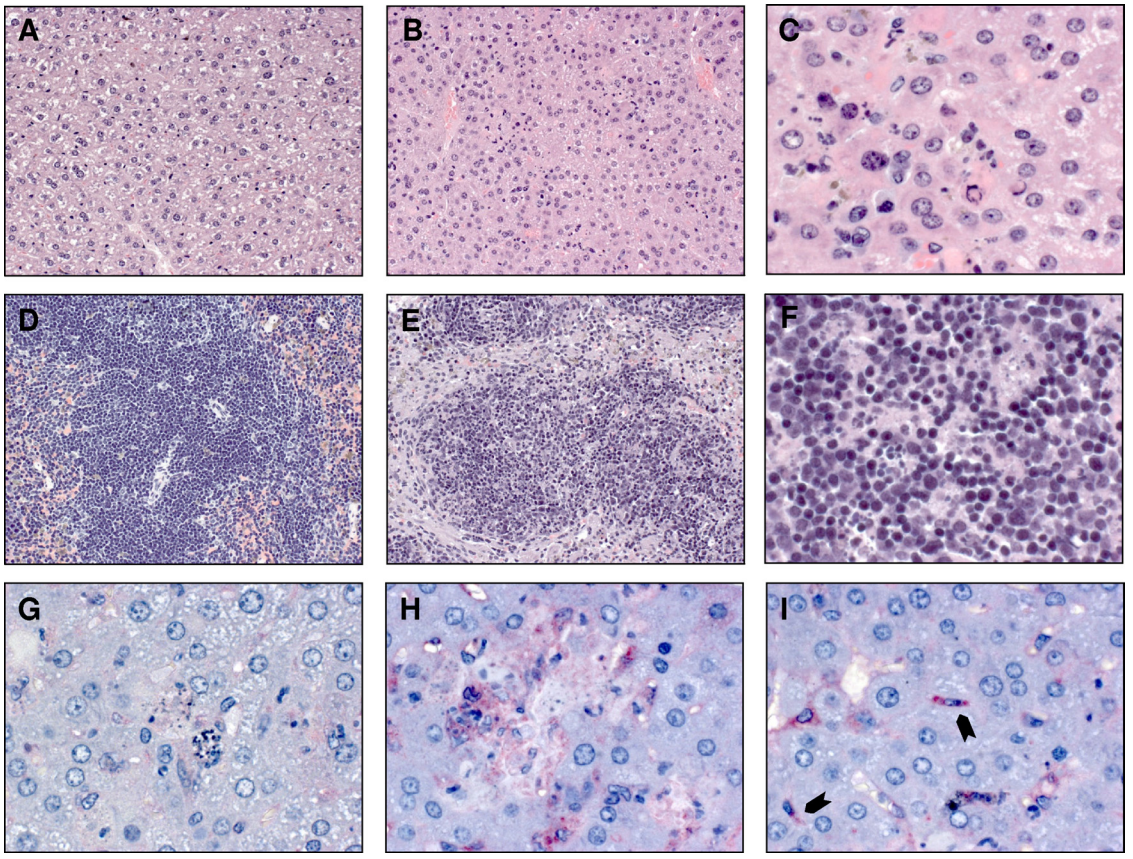

FIG. 4. Histopathologic changes were evident in liver and spleen of CCHFV-infected STAT129 mice. STAT129 mice were mock infected or inoculated intraperitoneally with 100 PFU of CCHFV IbAr 10200. Hematoxylin-and-eosin-stained sections of liver and spleen and IHC sections of liver of mice on day 3 postinfection are presented. Liver (A) and spleen (D) sections from mock-infected animals showed no histopathologic changes. The liver sections (B and C) showed multiple foci of hepatocellular necrosis. Original magnification was ×200 in panels A and B and ×630 in panel C. The spleen sections (E and F) showed prominent lymphocyte depletion and karyorrhectic debris. Original magnification was ×200 in panels D and E and ×630 in panel F. IHC assay was conducted with a polyclonal rabbit anti-CCHFV antibody. Negative control (G) showed no staining. Liver sections of infected animals (H and I) showed scattered granular staining (red) in foci of hepatocellular necrosis and occasional Kupffer cells (black arrows). Naphthol/fast red substrate with light hematoxylin counterstain were used; original magnification was ×200 in panels G and H and ×630 in panel I.

between 8 and 9 dpi. Ribavirin delayed the GMD in this group by 4.5 days compared to that for the control group challenged with 1,000 PFU of the virus. In order to develop reliable prognostic indicators, we assessed the clinical parameters, such as body temperature, weight change, and clinical scoring (Fig. 7C to E). Interestingly, survivors showed elevated temperature 1 day later than nonsurvivors and 2 days later than virus-only positive-control mice. Survivors also never became hypothermic (Fig. 7C). Weight loss was the same in virus-only mice, survivors, and nonsurvivors until 4 dpi. Nonsurvivors continued to lose weight, whereas survivors' weight leveled off for 3 days and then increased to reach the initial weight at 14 dpi. (Fig. 7D). Clinical scoring showed an initial period of sickness in survivors and nonsurvivors at 3 and 4 dpi. There were no clinical signs on days 5 and 6, but both survivors and nonsurvivors showed clinical signs on day 7. Survivors returned to a healthy state, whereas nonsurvivors succumbed to disease on days 8 and 9 postinfection (Fig. 7E).

None of the animals treated with ribavirin 24 h postinfection (treatment B) survived (Fig. 7A). However, in 40% of the animals in this group, GMD was delayed by 4.5 days to 7 days compared to that of the control mice.

When the animals were challenged with a virus dose of 10 PFU, all animals in both treatment group A and B survived (Fig. 7B). None of the animals exhibited clinical signs of disease or showed significant changes in temperature or weight compared to those of the treatment-only control group.

DISCUSSION

To measure the extent to which IFN-mediated antiviral responses control the virulence of CCHFV in mice, we evaluated CCHFV infection in mice lacking the STAT1 protein, a central component of the IFN signaling pathways. In the absence of the IFN response, CCHFV infection of STAT129 mice leads rapidly to disease and death. A low virus dose of 10 PFU results in 100% mortality, indicating the importance of the IFN response in controlling virus replication and dissemination in these animals. A more limited study using IFN receptor knockout mice demonstrated that mice succumb to CCHFV infec-

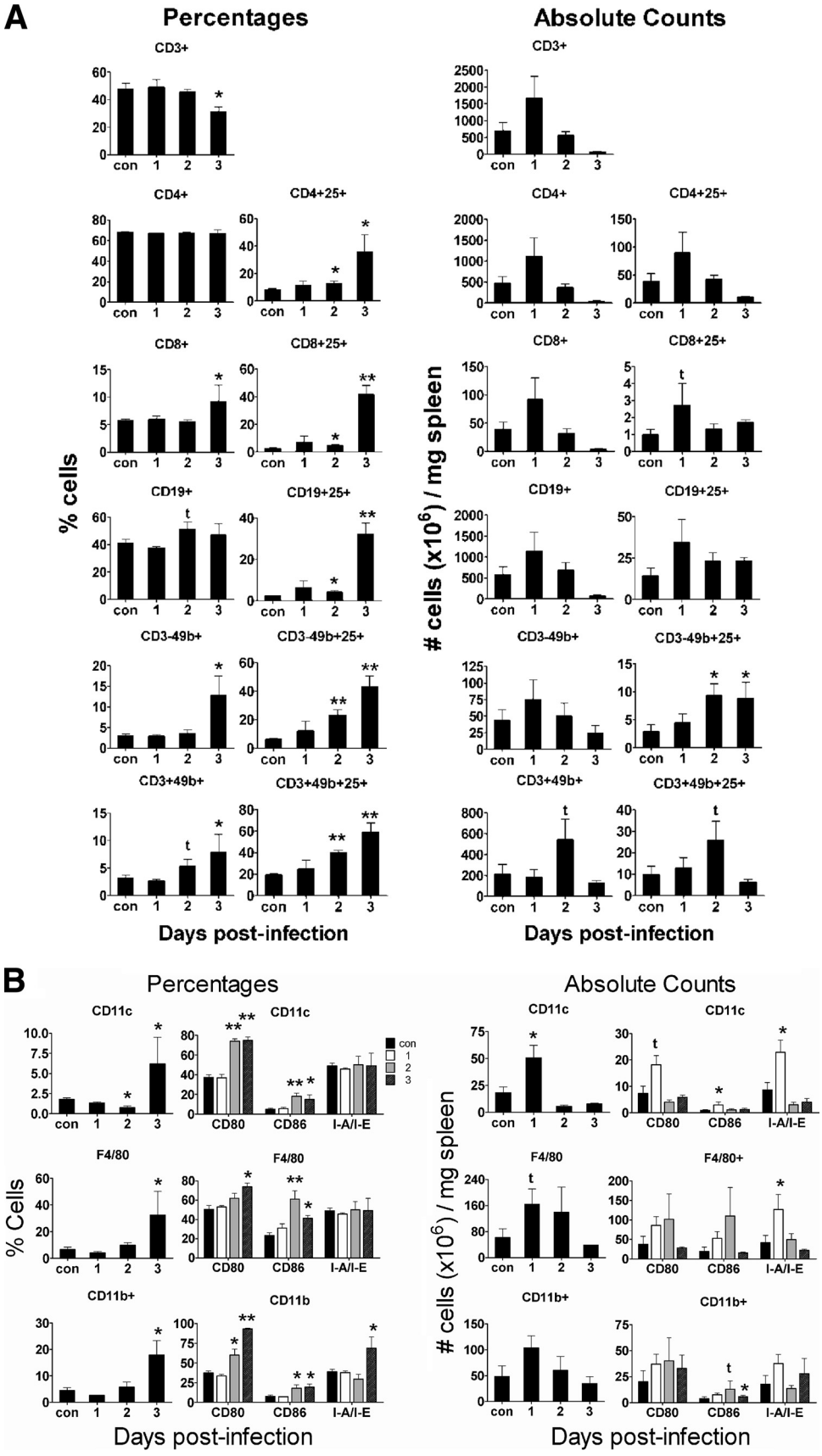
A
Percentages
Absolute Counts
CD3+
CD4+
CD4+25+
CD8+
CD8+25+
CD19+
CD19+25+
CD3-49b+
CD3-49b+25+
CD3+49b+
CD3+49b+25+
% cells
# cells (x10^6) / mg spleen
con 1 2 3
Days post-infection
B
Percentages
Absolute Counts
CD11c
F4/80
CD11b+
CD80
CD86
I-A/I-E
CD11b
% Cells
# cells (x10^6) / mg spleen
Days post-infection

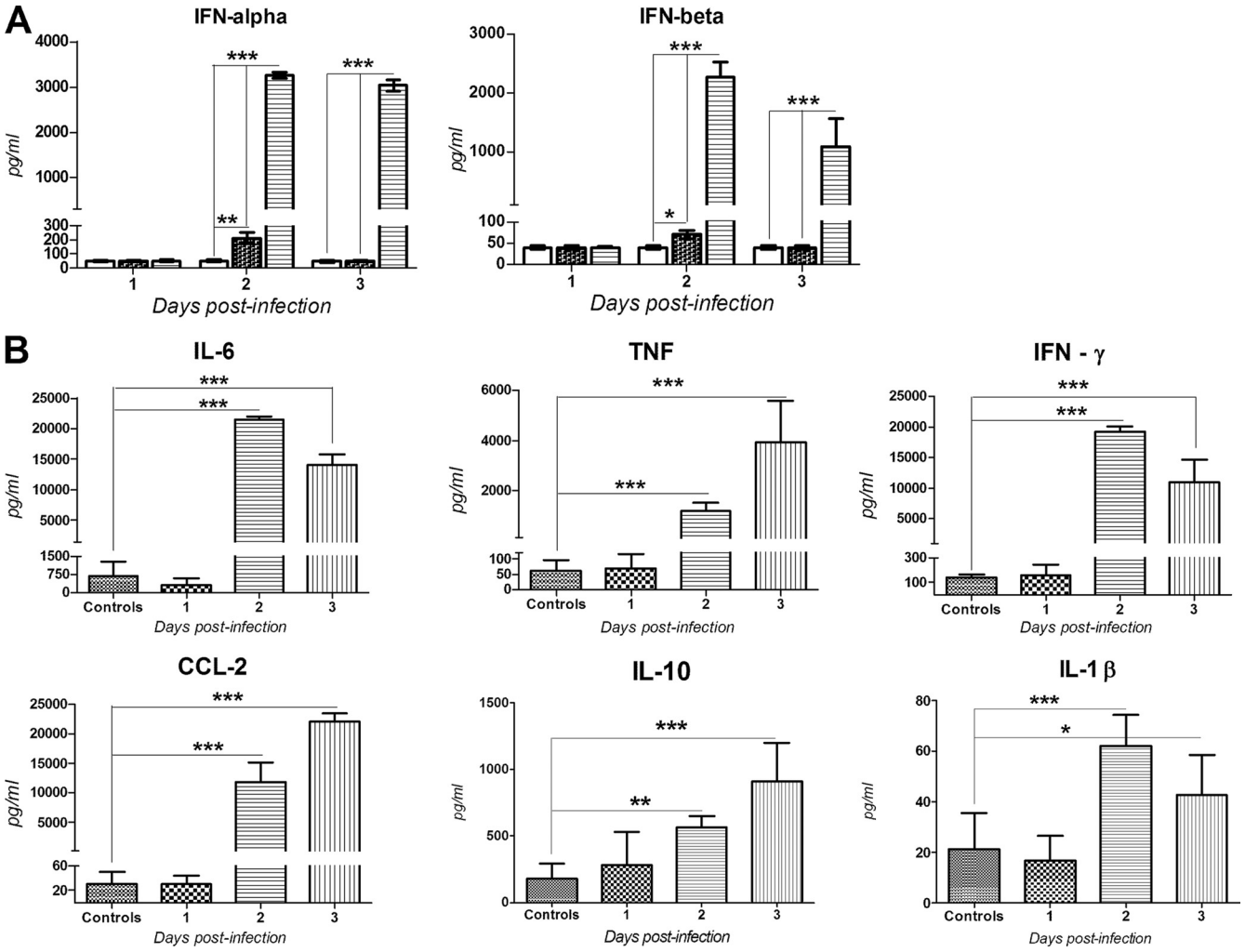

FIG. 6. IFN-α, IFN-β, and proinflammatory cytokines are elevated in infected animals on days 2 and 3 postinfection. (A) IFN-α and IFN-β levels were determined in plasma of mock-infected STAT129 mice (white bars), CCHFV-infected WT129 mice (checkered bars), and CCHFV-infected STAT129 mice (striped bars) and reported as pg/ml (mean + standard error). Unpaired *t* tests were performed between the results for mock-infected STAT129 mice and those for infected STAT129 and WT129 mice on each day postinfection. (B) Proinflammatory cytokines were measured in plasma of mock-infected STAT129 mice, CCHFV-infected WT129 mice, and CCHFV-infected STAT129 mice and reported as pg/ml (mean + standard error). Results for IL-6, TNF, IFN-γ, CCL-2, IL-10, and IL-1β in mock-infected and infected STAT129 mice are shown here. GM-CSF, IL-2, IL-4, and IL-12(p70) were not significantly elevated. No significant variation was detected in mock-infected animals between each time point; therefore, the results for the 3 time points were pooled (controls). Unpaired *t* tests were performed between the results for controls and the results for infected animals on each day postinfection. CCHFV-infected WT129 mice showed no significant differences in proinflammatory cytokine levels compared to the results for mock-infected STAT129 mice (data not shown).

tion with a similar GMD, providing supporting evidence that the IFN response is crucial for disease manifestation (5). In this study, high viral replication in CCHFV-infected STAT129 mice was present despite the high plasma levels of IFN-α and IFN-β, indicating that IFN is produced but unable to induce an IFN-mediated antiviral state due to the STAT1 knockout. We hypothesize that the ability of CCHFV to disable or evade components of the IFN response may be human specific. CCHFV infection of animals with a functional IFN antiviral response is, therefore, attenuated and does not cause disease in the animals.

CCHFV-infected STAT129 mice undergo an early burst of

FIG. 5. Changes in the leukocyte populations in the spleen during CCHFV infection. STAT129 mice were inoculated intraperitoneally with 100 PFU of CCHFV IbAr 10200. Spleens from mock-infected (control [con]) and CCHFV-infected mice were homogenized each day, and the various lymphocyte populations stained for immunophenotyping and activation levels and then analyzed by flow cytometry. The percentages and absolute counts for each population are shown. (A) Lymphocyte panel. (B) Macrophage and DC panel. Unpaired *t* tests were performed between the control samples and the infected samples on each day postinfection. Statistical symbols: ⋆, $P \leq 0.05$; ⋆⋆, $P \leq 0.001$; t indicates a trend where *P* is between 0.05 and 0.10.

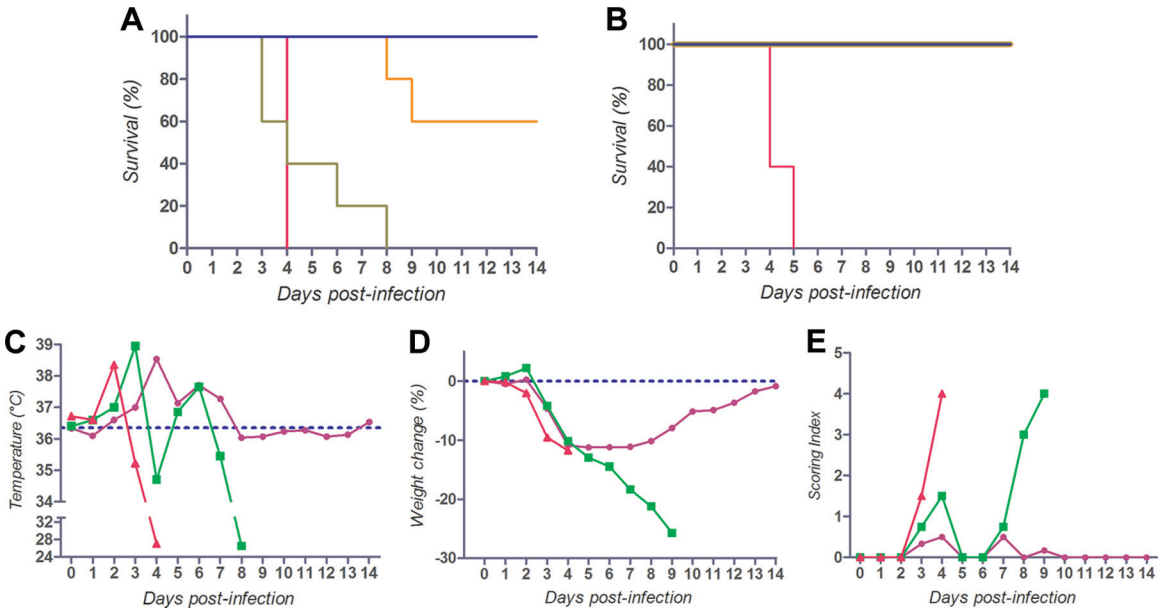

FIG. 7. Ribavirin protection study. (A and B) STAT129 mice were challenged i.p. with 1,000 PFU (A) or 10 PFU (B) of CCHFV IbAr 10200. Six animals per group received PBS (positive control; red), ribavirin treatment A (100 mg/kg, 1 h postinfection and then daily; orange), or ribavirin treatment B (100 mg/kg 24 h postinfection and then daily; green). Blue marks results for animals receiving ribavirin treatment A but no CCHFV. (C to E) Results for ribavirin treatment group A challenged with 1,000 PFU: survivors (purple) versus nonsurvivors (green) versus no-treatment group (red). Body temperature (C), weight change (D), and clinical scoring (E) were compared.

viral replication in the blood on day 1 postinfection and in liver and spleen on day 2 before virus disseminates systemically into multiple organs. The resulting high viremia levels in the blood on days 2 and 3 postinfection are comparable to severe disease in human cases (7, 36). In STAT129 mice, the liver and spleen are the major sites of replication and the only sites where prominent histopathologic changes were noticed. Interestingly, high CCHFV titers in spleen and low titers, late, in the brain were detected in some samples. This differs from the infant mouse model, which found high virus titers in the brain and none in the spleen (33). CCHFV in the model presented here exhibits hepatotropism, and the virus detected in the brain late in the infection is from blood-borne systemic spread rather than local replication. A subcutaneous inoculation would be a more relevant route when mimicking transmission by tick bite. A recent pilot study in our lab indicated that the subcutaneous route is still 100% lethal. However, the GMD was delayed by 1 day compared to the results for the same virus dose given by the i.p. route. Future studies will utilize this route of infection and compare the response to that seen with the i.p. route.

Clinical studies have demonstrated that thrombocytopenia, leukopenia, and raised levels of liver transaminases are hallmarks of CCHFV infection and can be used to predict fatal outcome in 90% of patients (20, 31). Similar changes in clinical chemistry and hematology can be found in the STAT129 mouse model, where white blood cell and platelet counts dropped on day 1 postinfection and reached their lowest values on day 2, while increasing slightly on day 3. At this point, further experiments are needed to determine if the leukopenia and thrombocytopenia are due to the migration of circulating white blood cells and platelets to infected organs or diminished production in and mobilization from the bone marrow. The more than 10-fold increase in ALT serum levels of CCHFV-infected animals by 3 dpi compared to the levels in mock-infected animals is a clear indicator of severe liver damage.

Histopathologic findings in CCHF cases are limited because histopathologic studies have been limited to a small number of human cases (6, 20). A spectrum of severity of hepatic damage was identified, ranging from mild necrosis with occasional Councilman bodies to more severe necrosis with extensive damage to hepatic lobules (6). The main findings in other tissues included prominent splenic lymphoid apoptosis and depletion and interstitial pneumonia. Except for the interstitial pneumonia, the histopathologic findings in this mouse model, particularly the association of CCHFV with Kupffer cells and hepatocytes, as well as prominent lymphocyte depletion in the spleen, reflect the findings in human cases. Hemorrhages, especially intestinal hemorrhaging, are often seen in human cases but were not found in this mouse model. This might be due to the rapid disease progression or differences in the murine coagulation cascade compared to that in humans.

Cytokines are major players in the pathogenesis of viral hemorrhagic fevers. In this study, we demonstrate that STAT129 mice respond to CCHFV infection with high levels of IFN-γ, IL-1β, IL-6, IL-10, CCL-2, and TNF on days 2 and 3 postinfection. IL-1β is a major mediator of innate immune reactions and is largely responsible for the acute-phase response, including fever and anorexia (9). CCL-2 is a marker of severe disease in murine and primate models of Ebola virus (17). In this model, IL-1β and CCL-2 peak on day 2 postinfection, with high levels on day 3, and correlate with viremia levels. We hypothesize that CCL-2 and IL-1β expression could enhance CCHFV infection by recruiting monocytes/macrophage cells to inflammatory sites early on and therefore in-

crease virus replication. IFN-γ is critical for innate and adaptive immunity against viral infections and is produced by NK cells and activated memory CTL cells (28). Therefore, high levels of IFN-γ on days 2 and 3 postinfection suggest a substantial activation of those cells. Recent clinical studies detected elevated levels of TNF, IL-6, and IL-10 in patients with CCHF (13, 25). Significantly higher levels of IL-6 and TNF were seen in CCHF patients with a fatal outcome than in nonfatal cases, whereas the IL-10 levels were not significantly different (13). In another study, high TNF levels correlated with the severity of CCHF disease, and the results suggested that IL-6 can be found in both mild and severe cases of CCHF (25). The results of these studies clearly signify the relevance of TNF, IL-6, and IL-10 in human CCHF cases, and the results presented here imply that they also play a critical role in the pathogenesis of our mouse model. IL-6 is a major cytokine of the acute-phase response and has been shown to raise body temperature, and TNF was shown to cause hypothermia in mice (21). Strikingly, IL-6 peaks on day 2 postinfection and TNF peaks on day 3, clearly coinciding with body temperature changes observed in animals. TNF production also contributes to macrophage activation, with resulting hemophagocytosis, and is correlated with the severity of other viral hemorrhagic fevers (16).

The changes in peripheral lymphocytes affected by CCHFV and their association with the severity of disease and mortality are very limited. However, evidence from human infections suggests immunological correlations with death. Two studies have looked at T, B, and NK cells in CCHF cases with contradicting results (1, 38). The first study correlated an increase in total NK numbers with severe cases of CCHF, where the highest NK cell counts occurred in fatal cases. In the second study, the NK cell counts were unchanged, while higher CTL counts correlated with both fatal cases and a higher viral load. However, this study looked at percentages and not absolute counts (38). In our study, the lymphocyte and APC populations in the spleen were activated within 3 dpi. The numbers of NK, B and T cells initially increased on day 1 postinfection, possibly influenced by early cytokine/chemokine production or other factors resulting from early viral replication in the spleen. However, the increases in absolute numbers were not sustained, and this was confirmed by the histopathological evidence of lymphocyte depletion in the spleen and leukopenia in the blood. This suggests that both the innate and adaptive immune systems may be sabotaged by the loss of leukocytes in the blood and spleen. However, since the STAT129 mice died by day 4 and there were no virus-specific IgM antibodies by 3 dpi in CCHFV-infected WT129 mice, clearly the innate immune system was unable to control the infection long enough for the adaptive immune response to ramp up. The percentage of activated NK cells increased up to day 3, but the absolute numbers showed the reverse trend, suggesting a loss of NK cells regardless of activation. This severely undermined the ability of the NK cells to control early viral replication. This may be due to CCHFV infecting primarily macrophages and DC (26). In addition to the loss of leukocytes, there is also some indication of a defective activation of immune cells. Our study demonstrates an insufficient upregulation of MHC-II in macrophages and DC that would be necessary for the correct activation of the adaptive immune response. Adequate levels of MHC-II are important for priming of naïve T cells; therefore, low MHC-II levels may contribute to the elimination of lymphocytes and hinder the ability to control the CCHFV infection.

Ribavirin is a synthetic purine nucleotide analog with a broad-spectrum antiviral activity that may be due to the alteration of the cellular nucleotide pools and inhibition of viral mRNA synthesis (19, 32). The effectiveness of ribavirin in CCHF cases has been described in a few observational studies (12, 15) that have been criticized for a lack of randomization and small sample size. Ribavirin significantly reduced mortality and extended GMD in a neonate mouse model (33). Here, we show that ribavirin protected 100% of STAT129 mice when challenged with 2.5 times the LD_{50} of CCHFV. Partial protection and extended GMD was achieved when animals were challenged with 250 times the LD_{50} and ribavirin was given early. Survivors showed delayed elevation in temperature compared to the results for nonsurvivors and untreated animals, suggesting delayed or lower viremia. When ribavirin was given 24 h postinfection, none of the animals survived, although GMD was delayed in 40% of the animals. Thus, the viremia levels at 24 h postinfection might already be too high to be significantly reduced by ribavirin. As a result, we hypothesize that the initial phase following CCHFV infection is crucial in controlling virus replication. Ribavirin may reach most of the primary cells infected in the abdominal cavity before systemic spread of the virus occurs, therefore reducing the initial virus load significantly. We did not measure viremia and virus titer in organs of infected STAT129 mice treated with ribavirin. Future work will show to what degree viremia and virus titers in organs are reduced after ribavirin treatment.

In conclusion, we have developed and characterized a new mature mouse model for CCHFV infection, allowing us to study the pathogenesis of this reemerging arbovirus. This study presents the first in-depth *in vivo* analysis of CCHFV pathophysiology and offers a validated small-animal model that exhibits key features of fatal human CCHF. This model may prove useful to study pathogenesis, test therapeutic strategies, and study virus attenuation.

ACKNOWLEDGMENTS

We thank Xiangguo Qiu and Anders Leung for animal care, Juno Lee for performing the quantitative RT-PCR of tissues, and Colette Keng (University of Texas Medical Branch, Galveston, TX) for help establishing the plaque assay.

Dennis Bente was funded by the Natural Sciences and Engineering Research Council of Canada (NSERC). The project received funding from the Public Health Agency of Canada (PHAC).

The funders had no role in study design, data collection and analysis, decision to publish, or preparation of the manuscript.

REFERENCES

1. **Akinci, E., M. Yilmaz, H. Bodur, P. Onguru, F. N. Bayazit, A. Erbay, and G. Ozet.** 2009. Analysis of lymphocyte subgroups in Crimean-Congo hemorrhagic fever. Int. J. Infect. Dis. **13:**560–563. doi:10.1016/j.ijid.2008.08.027.
2. **Akira, S.** 1999. Functional roles of STAT family proteins: lessons from knockout mice. Stem Cells **17:**138–146. doi:10.1002/stem.170138.
3. **Andersson, I., H. Karlberg, M. Mousavi-Jazi, L. Martinez-Sobrido, F. Weber, and A. Mirazimi.** 2008. Crimean-Congo hemorrhagic fever virus delays activation of the innate immune response. J. Med. Virol. **80:**1397–1404. doi:10.1002/jmv.21222.
4. **Andersson, I., A. Lundkvist, O. Haller, and A. Mirazimi.** 2006. Type I interferon inhibits Crimean-Congo hemorrhagic fever virus in human target cells. J. Med. Virol. **78:**216–222. doi:10.1002/jmv.20530.
5. **Bereczky, S., G. Lindegren, H. Karlberg, S. Akerstrom, J. Klingstrom, and**

A. Mirazimi. 2010. Crimean-Congo hemorrhagic fever virus infection is lethal for adult type I interferon receptor-knockout mice. J. Gen. Virol. **91:**1473–1477. doi:10.1099/vir.0.019034-0.

6. **Burt, F. J., R. Swanepoel, W. J. Shieh, J. F. Smith, P. A. Leman, P. W. Greer, L. M. Coffield, P. E. Rollin, T. G. Ksiazek, C. J. Peters, and S. R. Zaki.** 1997. Immunohistochemical and in situ localization of Crimean-Congo hemorrhagic fever (CCHF) virus in human tissues and implications for CCHF pathogenesis. Arch. Pathol. Lab. Med. **121:**839–846.
7. **Cevik, M. A., A. Erbay, H. Bodur, S. S. Eren, E. Akinci, K. Sener, P. Onguru, and A. Kubar.** 2007. Viral load as a predictor of outcome in Crimean-Congo hemorrhagic fever. Clin. Infect. Dis. **45:**e96–100. doi:10.1086/521244.
8. **Deyde, V. M., M. L. Khristova, P. E. Rollin, T. G. Ksiazek, and S. T. Nichol.** 2006. Crimean-Congo hemorrhagic fever virus genomics and global diversity. J. Virol. **80:**8834–8842. doi:10.1128/JVI.00752–06.
9. **Dinarello, C. A.** 1996. Biologic basis for interleukin-1 in disease. Blood **87:**2095–2147.
10. **Ergonul, O.** 2006. Crimean-Congo haemorrhagic fever. Lancet Infect. Dis. **6:**203–214. doi:10.1016/S1473-3099(06)70435-2.
11. **Ergonul, O.** 2008. Treatment of Crimean-Congo hemorrhagic fever. Antiviral Res. **78:**125–131. doi:10.1016/j.antiviral.2007.11.002.
12. **Ergonul, O.** 2009. Biases and misinterpretation in the assessment of the efficacy of oral ribavirin in the treatment of Crimean-Congo hemorrhagic fever. J. Infect. doi:10.1016/j.jinf.2009.08.006.
13. **Ergonul, O., S. Tuncbilek, N. Baykam, A. Celikbas, and B. Dokuzoguz.** 2006. Evaluation of serum levels of interleukin (IL)-6, IL-10, and tumor necrosis factor-alpha in patients with Crimean-Congo hemorrhagic fever. J. Infect. Dis. **193:**941–944. doi:10.1086/500836.
14. **Fagbami, A. H., O. Tomori, A. Fabiyi, and T. T. Isoun.** 1975. Experimantal Congo virus (Ib-AN 7620) infection in primates. Virologie **26:**33–37.
15. **Fisher-Hoch, S. P., J. A. Khan, S. Rehman, S. Mirza, M. Khurshid, and J. B. McCormick.** 1995. Crimean Congo-haemorrhagic fever treated with oral ribavirin. Lancet **346:**472–475.
16. **Fisman, D. N.** 2000. Hemophagocytic syndromes and infection. Emerg. Infect. Dis. **6:**601–608.
17. **Geisbert, T. W., L. E. Hensley, P. B. Jahrling, T. Larsen, J. B. Geisbert, J. Paragas, H. A. Young, T. M. Fredeking, W. E. Rote, and G. P. Vlasuk.** 2003. Treatment of Ebola virus infection with a recombinant inhibitor of factor VIIa/tissue factor: a study in rhesus monkeys. Lancet **362:**1953–1958. doi:10.1016/S0140-6736(03)15012-X.
18. **Gowen, B. B., and M. R. Holbrook.** 2008. Animal models of highly pathogenic RNA viral infections: hemorrhagic fever viruses. Antiviral Res. **78:**79–90. doi:10.1016/j.antiviral.2007.10.002.
19. **Graci, J. D., and C. E. Cameron.** 2006. Mechanisms of action of ribavirin against distinct viruses. Rev. Med. Virol. **16:**37–48. doi:10.1002/rmv.483.
20. **Joubert, J. R., J. B. King, D. J. Rossouw, and R. Cooper.** 1985. A nosocomial outbreak of Crimean-Congo haemorrhagic fever at Tygerberg Hospital. Part III. Clinical pathology and pathogenesis. S. Afr. Med. J. **68:**722–728.
21. **Leon, L. R., A. A. White, and M. J. Kluger.** 1998. Role of IL-6 and TNF in thermoregulation and survival during sepsis in mice. Am. J. Physiol. **275:** R269–R277.
22. **Meraz, M. A., J. M. White, K. C. Sheehan, E. A. Bach, S. J. Rodig, A. S. Dighe, D. H. Kaplan, J. K. Riley, A. C. Greenlund, D. Campbell, K. Carver-Moore, R. N. DuBois, R. Clark, M. Aguet, and R. D. Schreiber.** 1996. Targeted disruption of the Stat1 gene in mice reveals unexpected physiologic specificity in the JAK-STAT signaling pathway. Cell **84:**431–442.
23. **Morrill, J. C., G. B. Jennings, T. M. Cosgriff, P. H. Gibbs, and C. J. Peters.** 1989. Prevention of Rift Valley fever in rhesus monkeys with interferon-alpha. Rev. Infect. Dis. **11**(Suppl. 4)**:**S815–S825.
24. **Nalca, A., and C. A. Whitehouse.** 2007. Crimean-Congo hemorrhagic fever virus infection among animals, p. 155–165. *In* O. Ergonul and C. A. Whitehouse (ed.), Crimean-Congo hemorrhagic fever: a global perspective, 1st ed., Springer, Dordrecht, Netherlands.
25. **Papa, A., S. Bino, E. Velo, A. Harxhi, M. Kota, and A. Antoniadis.** 2006. Cytokine levels in Crimean-Congo hemorrhagic fever. J. Clin. Virol. **36:**272–276. doi:10.1016/j.jcv.2006.04.007.
26. **Peyrefitte, C. N., M. Perret, S. Garcia, R. Rodrigues, A. Bagnaud, S. Lacote, J. M. Crance, G. Vernet, D. Garin, M. Bouloy, and G. Paranhos-Baccala.** 2010. Differential activation profiles of Crimean-Congo hemorrhagic fever virus- and Dugbe virus-infected antigen-presenting cells. J. Gen. Virol. **91:** 189–198. doi:10.1099/vir.0.015701-0.
27. **Purnak, T., N. A. Selvi, and K. Altundag.** 2007. Global warming may increase the incidence and geographic range of Crimean-Congo hemorrhagic fever. Med. Hypotheses **68:**924–925. doi:10.1016/j.mehy.2006.09.020.
28. **Schoenborn, J. R., and C. B. Wilson.** 2007. Regulation of interferon-gamma during innate and adaptive immune responses. Adv. Immunol. **96:**41–101. doi:10.1016/S0065-2776(07)96002-2.
29. **Shepherd, A. J., P. A. Leman, and R. Swanepoel.** 1989. Viremia and antibody response of small African and laboratory animals to Crimean-Congo hemorrhagic fever virus infection. Am. J. Trop. Med. Hyg. **40:**541–547.
30. **Smirnova, S. E.** 1979. A comparative study of the Crimean hemorrhagic fever-Congo group of viruses. Arch. Virol. **62:**137–143.
31. **Swanepoel, R., D. E. Gill, A. J. Shepherd, P. A. Leman, J. H. Mynhardt, and S. Harvey.** 1989. The clinical pathology of Crimean-Congo hemorrhagic fever. Rev. Infect. Dis. **11**(Suppl. 4)**:**S794–S800.
32. **Tam, R. C., J. Y. Lau, and Z. Hong.** 2001. Mechanisms of action of ribavirin in antiviral therapies. Antivir. Chem. Chemother. **12:**261–272.
33. **Tignor, G. H., and C. A. Hanham.** 1993. Ribavirin efficacy in an in vivo model of Crimean-Congo hemorrhagic fever virus (CCHF) infection. Antiviral Res. **22:**309–325.
34. **Watts, D. M., M. A. Ussery, D. Nash, and C. J. Peters.** 1989. Inhibition of Crimean-Congo hemorrhagic fever viral infectivity yields in vitro by ribavirin. Am. J. Trop. Med. Hyg. **41:**581–585.
35. **Whitehouse, C. A.** 2004. Crimean-Congo hemorrhagic fever. Antiviral Res. **64:**145–160. doi:10.1016/j.antiviral.2004.08.001.
36. **Wolfel, R., J. T. Paweska, N. Petersen, A. A. Grobbelaar, P. A. Leman, R. Hewson, M. C. Georges-Courbot, A. Papa, S. Gunther, and C. Drosten.** 2007. Virus detection and monitoring of viral load in Crimean-Congo hemorrhagic fever virus patients. Emerg. Infect. Dis. **13:**1097–1100.
37. **Woodall, J. P., M. C. Williams, and D. I. Simpson.** 1967. Congo virus: a hitherto undescribed virus occurring in Africa. II. Identification studies. East Afr. Med. J. **44:**93–98.
38. **Yilmaz, M., K. Aydin, E. Akdogan, N. Sucu, M. Sonmez, S. B. Omay, and I. Koksal.** 2008. Peripheral blood natural killer cells in Crimean-Congo hemorrhagic fever. J. Clin. Virol. **42:**415–417. doi:10.1016/j.jcv.2008.03.003.